Schematic Analysis and Fiducial Point of Tooth for Root Canal Therapy

Dooyeol Kim
Department of Orthodontics, The University of Texas Health Science Center at Houston, School of Dentistry

Mustafa Aldabbagh
Department of Endodontics, The University of Texas Health Science Center at Houston, School of Dentistry

Scott R. Makins
Department of Endodontics, The University of Texas Health Science Center at Houston, School of Dentistry

Helder B. Jacob
Department of Orthodontics, The University of Texas Health Science Center at Houston, School of Dentistry

Julian N. Holland
Office of Research, The University of Texas Health Science Center at Houston, School of Dentistry

Ji Wook Jeong (ji.wook.jeong@uth.tmc.edu)
Department of Endodontics, The University of Texas Health Science Center at Houston, School of Dentistry

Research Article

Keywords: Collum angle, endodontic access, fiducial point, root canal axis, tangent angle

Posted Date: July 21st, 2022

DOI: https://doi.org/10.21203/rs.3.rs-1836541/v1

Abstract

Objectives To identify schematic relationships between root canal axis, the cementoenamel junction (CEJ), and the contour of the clinical crown's facial surface in maxillary central incisors.

Materials and Methods 72 radiographic images of extracted maxillary central incisors with previous root canal treatment were collected. Angles (tangent angle) between the root canal axis and lines tangent to fiducial points on the facial surface 3.5 mm, 4.0 mm, 4.5 mm, 5.0 mm, and 5.5 mm cervical to the incisal edge were measured using ImageJ software. Facial-palatal CEJ widths were measured and divided into facial and palatal CEJ by the root canal axis. Generalized linear models were used to assess any relationship between CEJ widths and the constructed tangent angles. The Paired Difference T-test was performed to determine the ratio of palatal CEJ to facial CEJ widths.

Results The correlation between CEJ width and angle measurements was statistically significant except at 3.5 mm ($P < .05$). The tangent angle values decreased from the most incisal point (22.8°) to the most cervical point (18.4°). The average value of total CEJ widths was 7.44 mm. Palatal CEJ was on average 0.22 mm greater than facial CEJ widths ($P = 1.61e^{-6}$).

Conclusions Using CEJ width and tangent angle of fiducial point, the root canal axis of the maxillary central incisor can be predicted.

Clinical relevance Crown morphology can be applied to design a standardized endodontic access stent to aid in root canal therapy in maxillary central incisors when the canal is difficult to identify.

Introduction

Partial or total obliteration of the pulp spaces as a consequence of tooth trauma ranges from 4 to 64% [1–4] and usually affects the anterior teeth of young people, particularly the maxillary central incisor [5]. Pulp canal obliteration (PCO) commonly occurs in teeth with incomplete root formation following an extrusion, lateral luxation, or intrusion injury as the response of vital pulp tissue to severe injury [2]. PCO also occurs as a healing mechanism following the reimplantation of avulsed immature permanent teeth [6] as the open apex of an immature tooth allows re-establishment of the blood supply and subsequent deposition of tertiary dentin following avulsion [7]. Clinically, PCO is associated with yellow discoloration or reduced translucency of the clinical crown in approximately 75% of cases [1, 4, 8]. Radiographically, PCO presents as loss or severe reduction of the pulp space (Fig. 1).

As only a small percentage of teeth with PCO develop pulp necrosis, prophylactic root canal therapy (RCT) is not indicated [1, 5]. Endodontic therapy is only indicated for teeth with PCO that have tenderness to percussion, a moderate to high periapical index (PAI) score, and a negative response to sensibility testing [1, 8]. Each category of the PAI represents a degree of periapical inflammation, and a moderate to high score (PAI $\geq$ 3) is characterized by changes in periapical bone structure with some mineral loss,

associated pain on percussion or spontaneous pain, and intraoral findings ranging from a draining sinus tract to slight soft tissue swelling [8, 9].

When RCT is indicated, PCO presents unique treatment challenges. Teeth with PCO fall into the High Difficulty category for treatment according to the American Association of Endodontists Case Assessment criteria [10]. Achieving proper access for RCT can be extremely challenging due to the narrowing or obliteration of the pulp chamber, leading to complications such as root perforation or irretrievable instrument fracture [5]. Recently, guided access methodologies using custom stents produced by 3D-printing or a complex navigation system [11–14] represent methodologies to reduce PCO-related complications during RCT. However, these techniques require cone-beam computerized tomography (CBCT) images to facilitate the printing of customized stents or orientation of the navigation system. The necessary multiple prerequisite steps, complex instrumentarium, and required software associated with these methods also increases the time and cost of endodontic treatment of teeth exhibiting PCO.

Currently, there is not a preprogrammed standardized endodontic stent available for initiating root canal therapy of maxillary incisors with PCO. The clinician must take periapical radiographic images at multiple angles to assess and maintain the ideal alignment of the access from the pulp chamber to the root canal orifice [15] or utilize the aforementioned custom methodologies. Fabrication of a standardized access stent requires determining if consistent physical relationships exist between the orientation of the clinical crown, the long axis of the root, and the location of the canal's coronal orifice.

Findings from previous studies concerning morphologic relationships of maxillary anterior teeth can be utilized to design a technique for endodontic access of such teeth exhibiting PCO. The inclination between the long axis of the clinical crown and that of the root for maxillary incisors is known as the Collum angle, and it consistently equates to approximately 5 degrees [16–19]. We have hypothesized that a location of *fiducial point* cervical to the incisal edge of the maxillary central incisor and its associated tangent angle are schematically related to the root canal's long axis. Orthodontics related studies have shown labial brackets can be positioned more appropriately by measuring their location in relation to the incisal edge rather than the center of the clinical crown [20]. Also, the crowns' long axes of most patients are consistently related to the facial or buccal surface morphology of those crowns [21]. The cementoenamel junction (CEJ) width can be used to estimate the location of the root canal orifice as the orifice is essentially located in the center of the root [22]. Having determined the location of the canal orifice in relation to the root's facial and palatal surfaces, the long axis of the canal space can be established.

The goal of this study was to identify schematic relationships between the root canal axis, the facial-palatal CEJ width, and the contour of the clinical crown's facial surface for maxillary central incisors. Data was derived from cross sectional, periapical radiographic images of multiple maxillary incisors. Establishing these relationships will make it possible to design a standardized endodontic access stent

for use with maxillary incisors displaying PCO, thereby eliminating the need for CBCT images, custom positioning devices or specialized software.

Materials And Methods

Proximal radiographic images of 91 extracted maxillary central incisor teeth were collected from predoctoral students' simulation laboratory projects. Images presenting two lingual outlines were excluded as this indicated the teeth were not mounted with the tooth's mesiodistal axis in line with the X-ray beam's central ray. 72 images satisfied the selection criteria. ImageJ software (ImageJ, U.S. National Institutes of Health, Bethesda, MD, USA; downloadable at https://imagej.nih.gov/ij/) was used to analyze the tooth morphology relationships of interest within the radiographs. The long axis of each root canal was determined by locating the center of the root canal space in the coronal-third and in the middle-third of the root (Fig. 2). The apical-third of the roots were disregarded because of the prevalent curvature of the canal in that region [23, 24].

To establish consistent and reproducible locations of *fiducial points* on the facial surface of the clinical crown cervical to the incisal edge, the following protocol was developed (Fig. 2A). First, a line was drawn from the incisal edge to the most prominent cervical bulge (I-C line). On the I-C line, the location 3.5 mm cervical to the incisal edge was identified. A perpendicular line was drawn from this location on the I-C line to the facial surface and a line tangent to the facial surface at the intersection was drawn. The angle between the root canal long axis and the tangent line (tangent angle) was recorded. This was repeated for the *fiducial point* locations of 4.0 mm, 4.5 mm, 5.0 mm, and 5.5 mm cervical to the incisal edge for each of the 72 radiographic images.

Second, the facial-palatal cementoenamel junction widths were measured (Fig. 2B). A line was drawn from the radiographic facial CEJ to the radiographic palatal CEJ. The root canal axis line intersecting the CEJ line was used to delineate facial CEJ width and palatal CEJ width dimensions at each of the five levels. The total facial-palatal CEJ width was also recorded.

Statistical analysis was performed using R statistical software (R Foundation for Statistical Computing, Vienna, Austria. URL https://www.Rproject.org/). Generalized linear models were used to assess any relationship between CEJ widths and the constructed tangent angles. The Paired Difference T-test was performed to determine the ratio of palatal CEJ widths to facial CEJ widths, with the level of significance set at $P < 0.05$.

Results

The correlations between the CEJ widths and tangent angles were statistically significant for the tangent lines drawn at the *fiducial points* 4.0 mm, 4.5 mm, 5.0 mm, and 5.5 mm cervical to the incisal edge. The R^2 values for these locations were 0.068, 0.064, 0.061, and 0.055, respectively (Table 1). The tangent angles displaying the narrowest distribution plots were those closer to the center of the crown's facial

curvature. The tangent angle values decreased from the most incisal *fiducial point* location to the most cervical location. At 5.5 mm cervical from the incisal edge, the average tangent angle was approximately 20% less than the average tangent angle at 3.5 mm. Similar results have been shown in other studies [25].

Total facial-palatal CEJ widths (facial surface – palatal surface) had an average value of 7.44 mm, standard deviation of 0.611 mm, minimum value of 6.30 mm, and maximum value of 8.92 mm. Facial CEJ width (facial surface – canal orifice) had an average value of 3.61 mm, standard deviation of 0.339 mm, minimum value of 2.91 mm, and maximum value of 4.28 mm. Palatal CEJ width (palatal surface – canal orifice) had an average value of 3.83 mm, standard deviation of 0.365 mm, minimum value of 3.03 mm, and maximum value of 4.92 mm. Paired Difference T-test between palatal and facial CEJ width produced a T-value of 5.23, with degrees of freedom of 71, and a *P*-value of $1.61e^{-6}$. The 95% confidence interval was 0.133 mm to 0.296 mm, and the Mean of the differences was 0.214 mm (Table 2).

Discussion

The objective of this study was to determine if geometric relationships exist between the clinical crown morphology and the long axis of the root canal that would enable designing of a standardized access stent for endodontic treatment of maxillary incisors with pulp canal obliteration (PCO). On average, the anatomic crown height of the maxillary central incisor is approximately 12 mm with unworn incisal edges and 11 mm with worn edges [26]. Although the maxillary central incisor crown shows some facial contour variation, it serves as a more consistent reference structure for determining crown-to-root angulation due to the greater variation in shape of the root.

The results of this study indicate that the relationships between the facial-palatal CEJ widths and the tangent angles at 4.0 mm, 4.5 mm, 5.0 mm, and 5.5 mm cervical to the incisal edge are significantly correlated (Fig. 3, Table 1). The mid-point at 4.5 mm presented the least variation (standard deviation 5.25 degrees), indicating it has potential as a landmark for the design of a standardized access stent. Of the four statistically significant locations, 5.5 mm produced the most variation, standard deviation 5.41 degrees, and is less desirable as a beneficial reference point. Palatal CEJ widths were on average 0.22 mm greater than facial CEJ widths, with a *P*-value of $1.61e^{-6}$. This result indicates that the root canal axis is not centered at the facial-palatal CEJ, but displaced slightly towards the facial CEJ. Using the statistical results, the authors generated the formulas as below.

- tangent angle ∝ CEJ width
- distance between *fiducial point* and incisal edge ∝ 1 / tangent angle
- palatal CEJ width = facial CEJ width + 0.2 mm

The programmed access stent can be designed based on these formulas. The clinician can measure the CEJ width and locate the *fiducial point* for proper stent application. However, it is necessary to increase

the sample size in order to obtain more repeatable values of the tangent angle in relation to CEJ width in the future.

A limitation of the results lies in the R^2 values. Our statistically significant results at 4.0 mm, 4.5 mm, 5.0 mm, and 5.5 mm cervical to the incisal edge produced R^2 values of 0.068, 0.064, 0.061, and 0.055, respectively. This means that at 4.0 mm cervical to the incisal edge, this study explains only 6.8% of variability around the mean; at 4.5 mm cervical to the incisal edge, this study explains only 6.4% of variability around the mean, and so on. Although these results are statistically significant, they do not fully account for the variability seen in these samples. There may be other factors influencing the relationship between CEJ width and angle measurement. For example, variation in human tooth size and morphology may play a role in the low R^2 values. Previous studies have shown that patients with Class II Division 2 Angle classification had larger Collum angles than those of other classifications [16–19]. Because the radiographic images in this study were of de-identified natural teeth, it was not possible to determine the Angle classification of the original dentition.

In summary, the data revealed a significant correlation between the CEJ width and the tangent angles plotted at the *fiducial points* 4.0 mm, 4.5 mm, 5.0 mm, and 5.5 mm cervical to the incisal edge. This relationship can be used to predict the location of the root canal orifice and the orientation of the canal's long axis in maxillary central incisors. Additionally, this study found the root canal long axis and the canal orifice, tend to be displaced slightly towards the facial portion of the root. Determining the location of the canal orifice and the orientation of root canal's long axis is essential prior to beginning RCT for maxillary central incisors with PCO where the clinician may otherwise experience difficulty accessing the crown and successfully locating the canal without the possible complications of crown or root perforation. The authors suggest the data from this study can be applied to design a standardized access stent for generating appropriate RCT access openings in maxillary anterior teeth presenting with PCO and requiring endodontic treatment.

Declarations

Author contribution Dooyeol Kim contributed to design, data acquisition, analysis and interpretation, drafted and critically revised the manuscript. Prepared figures 1- 3 and tables 1-2. Mustafa Aldabbagh contributed to data acquisition and analysis. Prepared figures 2. Scott R. Makins contributed to conception, design, critically revised the manuscript. Critically revised figures 2- 3 and tables 1-2. Helder B. Jacob contributed to data interpretation and critically revised the manuscript. Critically revised tables 1-2. Julian N. Holland contributed to data analysis and interpretation. Critically revised figures 3 and tables 1-2. Ji Wook Jeong contributed to conception, design, data interpretation and critically revised the manuscript. Critically prepared and revised figures 1- 3 and tables 1-2.

Funding No funding was obtained for this study.

Ethical approval This article does not contain any studies with human participants or animals performed by any of the authors

Informed consent For this type of study, formal consent is not required.

Conflict of interest The authors declare no competing interests.

References

1. Robertson A, Andreasen FM, Bergenholtz G, Andreasen JO, Norén JG (1996) Incidence of pulp necrosis subsequent to pulp canal obliteration from trauma of permanent incisors. J Endod 22:557-560. https://doi.org/10.1016/S0099-2399(96)80018-5
2. Andreasen FM, Zhijie Y, Thomsen BL, Andersen PK (1987) Occurrence of pulp canal obliteration after luxation injuries in the permanent dentition. Endod Dent Traumatol 3:103-115. https://doi.org/10.1111/j.1600-9657.1987.tb00611.x
3. Holcomb JB, Gregory WB, Jr (1967) Calcific metamorphosis of the pulp: its incidence and treatment. Oral Surg Oral Med Oral Pathol 24:825-830. https://doi.org/10.1016/0030-4220(67)90521-X
4. Jacobsen I, Kerekes K (1977) Long-term prognosis of traumatized permanent anterior teeth showing calcifying processes in the pulp cavity. Scand J Dent Res 85:588-598. https://doi.org/10.1111/j.1600-0722.1977.tb02119.x
5. McCabe PS, Dummer PM (2012) Pulp canal obliteration: an endodontic diagnosis and treatment challenge. Int Endod J 45:177-197. https://doi.org/10.1111/j.1365-2591.2011.01963.x
6. Abd-Elmeguid A, ElSalhy M, Yu DC (2015) Pulp canal obliteration after replantation of avulsed immature teeth: a systematic review. Dent Traumatol 31:437-441. https://doi.org/10.1111/edt.12199
7. Yanpiset K, Vongsavan N, Sigurdsson A, Trope M (2001) Efficacy of laser Doppler flowmetry for the diagnosis of revascularization of reimplanted immature dog teeth. Dent Traumatol 17:63-70. https://doi.org/10.1034/j.1600-9657.2001.017002063.x
8. Oginni AO, Adekoya-Sofowora CA, Kolawole KA (2009) Evaluation of radiographs, clinical signs and symptoms associated with pulp canal obliteration: an aid to treatment decision. Dent Traumatol 25:620-625. https://doi.org/10.1111/j.1600-9657.2009.00819.x
9. Ørstavik D, Kerekes K, Eriksen HM (1986) The periapical index: a scoring system for radiographic assessment of apical periodontitis. Endod Dent Traumatol 2:20-34. https://doi.org/10.1111/j.1600-9657.1986.tb00119.x
10. American Association of Endodontists (2022) AAE Endodontic Case Difficulty Assessment Form and Guidelines. Available from https://www.aae.org/specialty/clinical-resources/treatment-planning/case-assessment-tools/ Accessed April 2022.
11. Anderson J, Wealleans J, Ray J (2018) Endodontic applications of 3D printing. Int Endod J 51:1005-1018. https://doi.org/10.1111/iej.12917

12. Jain SD, Saunders MW, Carrico CK, Jadhav A, Deeb JG, Myers GL (2020) Dynamically Navigated versus Freehand Access Cavity Preparation: A Comparative Study on Substance Loss Using Simulated Calcified Canals. J Endod 46:1745-1751. https://doi.org/10.1016/j.joen.2020.07.032
13. Dianat O, Nosrat A, Tordik PA, Aldahmash SA, Romberg E, Price JB, Mostoufi B (2020) Accuracy and Efficiency of a Dynamic Navigation System for Locating Calcified Canals. J Endod 46:1719-1725. https://doi.org/10.1016/j.joen.2020.07.014
14. Connert T, Leontiev W, Dagassan-Berndt D, Kuhl S, ElAyouti A, Krug R, Krastl G, Weiger R (2021) Real-Time Guided Endodontics with a Miniaturized Dynamic Navigation System Versus Conventional Freehand Endodontic Access Cavity Preparation: Substance Loss and Procedure Time. J Endod 47:1651-1656. https://doi.org/10.1016/j.joen.2021.07.012
15. O'Connor RP, De Mayo TJ, Roahen JO (1994) The lateral radiograph: an aid to labiolingual position during treatment of calcified anterior teeth. J Endod 20:183-184. https://doi.org/10.1016/S0099-2399(06)80332-8
16. Khalid Z, Iqbal K, Khalid S, Riaz A, Jan A (2020) Comparison of Collum Angle of Maxillary Central Incisors in Different Incisor Relationships. J Coll Physicians Surg Pak 30:471-475. https://doi.org/10.29271/jcpsp.2020.05.471
17. Feres MFN, Rozolen BS, Alhadlaq A, Alkhadra TA, El-Bialy T (2018) Comparative tomographic study of the maxillary central incisor collum angle between Class I, Class II, division 1 and 2 patients. J Orthod Sci 7:6. https://10.4103/jos.JOS_84_17
18. Srinivasan B, Kailasam V, Chitharanjan A, Ramalingam A (2013) Relationship between crown-root angulation (collum angle) of maxillary central incisors in Class II, division 2 malocclusion and lower lip line. Orthodontics: The Art and Practice of Dentofacial Enhancement 14:e66-74. https://doi.org/10.11607/ortho.841
19. Elangovan B, Srinivasan B, Kailasam V, Padmanabhan S (2020) Comparison of the collum angle of incisors and canines in skeletal malocclusions - A CBCT study. Int Orthod 18:468-479. https://doi.org/10.1016/j.ortho.2020.06.006
20. Armstrong D, Shen G, Petocz P, Darendeliler MA (2007) A comparison of accuracy in bracket positioning between two techniques--localizing the centre of the clinical crown and measuring the distance from the incisal edge. Eur J Orthod. 29:430-436. https://doi.org/10.1093/ejo/cjm037
21. Andrews LF (1972) The six keys to normal occlusion. Am J Orthod 62:296-309. https://doi.org/10.1016/S0002-9416(72)90268-0
22. Krasner P, Rankow HJ (2004) Anatomy of the pulp-chamber floor. J Endod 30:5-16. https://doi.org/10.1097/00004770-200401000-00002
23. Schäfer E, Diez C, Hoppe W, Tepel J (2002) Roentgenographic investigation of frequency and degree of canal curvatures in human permanent teeth. J Endod 28:211-216. https://doi.org/10.1097/00004770-200203000-00017
24. Kasahara E, Yasuda E, Yamamoto A, Anzai M (1990) Root canal system of the maxillary central incisor. J Endod 16:158-161. https://10.7759/cureus.7851

25. Kong WD, Ke JY, Hu XQ, Zhang W, Li SS, Feng Y (2016) Applications of cone-beam computed tomography to assess the effects of labial crown morphologies and collum angles on torque for maxillary anterior teeth. Am J Orthod Dentofacial Orthop 150:789-795. https://doi.org/10.1016/j.ajodo.2016.03.029
26. Magne P, Gallucci GO, Belser UC (2003) Anatomic crown width/length ratios of unworn and worn maxillary teeth in white subjects. J Prosthet Dent 89:453-461. https://doi.org/10.1016/S0022-3913(03)00125-2

Tables

Table 1 Average tangent angle measurements, standard deviations, *P*-values, and R2 values at 3.5 mm, 4.0 mm, 4.5 mm, 5.0 mm, 5.5 mm cervical to the incisal edge. The relationship between CEJ width and locations 4.0 mm, 4.5 mm, 5.0 mm, and 5.5 mm cervical to the incisal edge were statistically significant. Values within different superscript letters within each column have statistically significant differences ($P < 0.05$)

Distance from incisal edge	Average tangent angle (degrees)	Standard deviation (degrees)	Relationship to CEJ width (*P*-value)	R2 value
3.50 mm	22.8A	5.32	.055	0.051
4.00 mm	21.7A,B	5.37	.027*	0.068
4.50 mm	20.6B,C,D	5.25	.032*	0.064
5.00 mm	19.4C,D	5.39	.037*	0.061
5.50 mm	18.4D	5.41	.047*	0.055

Table 2 Average values, standard deviations, minimum values, and maximum values for total CEJ width, facial CEJ width, and palatal CEJ width. Paired Difference T-test between palatal and facial CEJ width resulted in T-value = 5.23, df = 71, *P*-value = 1.61-6, 95% confidence interval = 0.133 mm to 0.296 mm, mean of differences = 0.214mm

	Average value (mm)	Standard deviation (mm)	Minimum value (mm)	Maximum value (mm)
Total CEJ width	7.44	0.611	6.30	8.92
Facial CEJ width	3.61	0.339	2.91	4.28
Palatal CEJ width	3.83	0.365	3.03	4.92

Figures

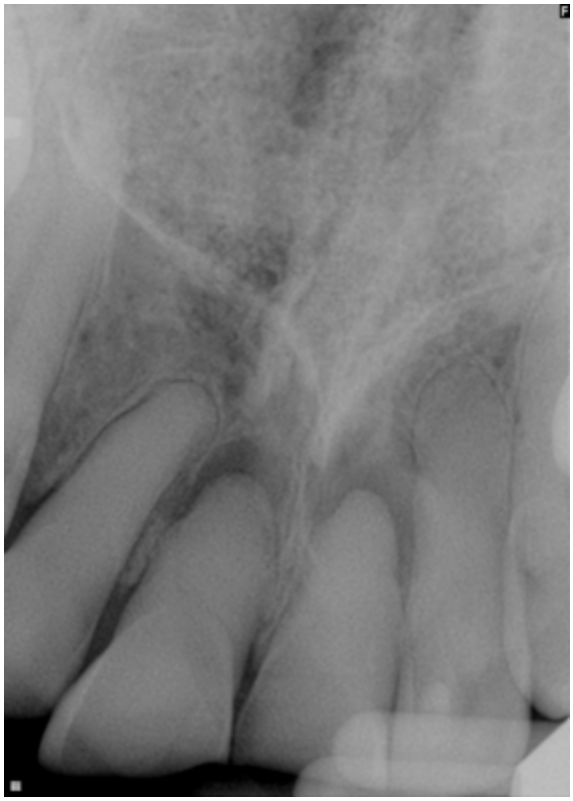

Figure 1

Periapical radiograph of pulp canal obliteration in maxillary central incisors. Pulp canal obliteration is characterized by the inability to identify the pulp canal on radiographic exam

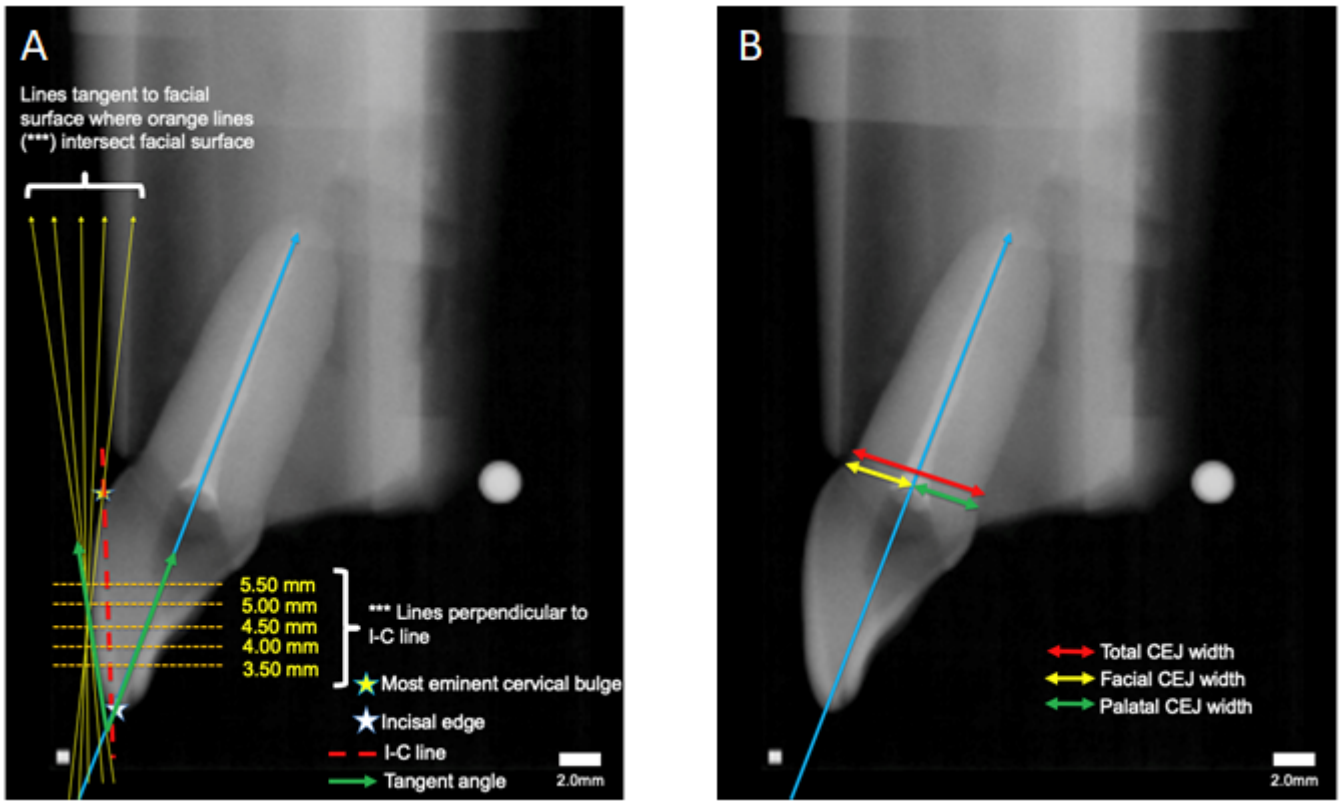

Figure 2

Diagrams of radiographic measurements. (**A**) Sample measurements of root canal axis, lines tangent to facial surface, and tangent angle. White star represents incisal edge, and yellow star represents most eminent cervical bulge. Blue line represents the root canal axis. Red line represents line from incisal edge to most eminent cervical bulge (I-C line). Orange lines represent lines perpendicular to the I-C line at 3.5 mm, 4.0 mm, 4.5 mm, 5.0 mm, and 5.5 mm cervical to the incisal edge. Yellow lines represent lines tangent to the facial surface where orange lines intersect facial surface. Green arrows represent angle measurement collected between lines tangent to the facial surface and root canal axis (tangent angle). (**B**) Sample CEJ width measurement. Blue line represents root canal axis. Red line represents total CEJ width. Yellow line represents facial CEJ, and green line represents palatal CEJ. Facial and palatal CEJ were delineated by the root canal axis line

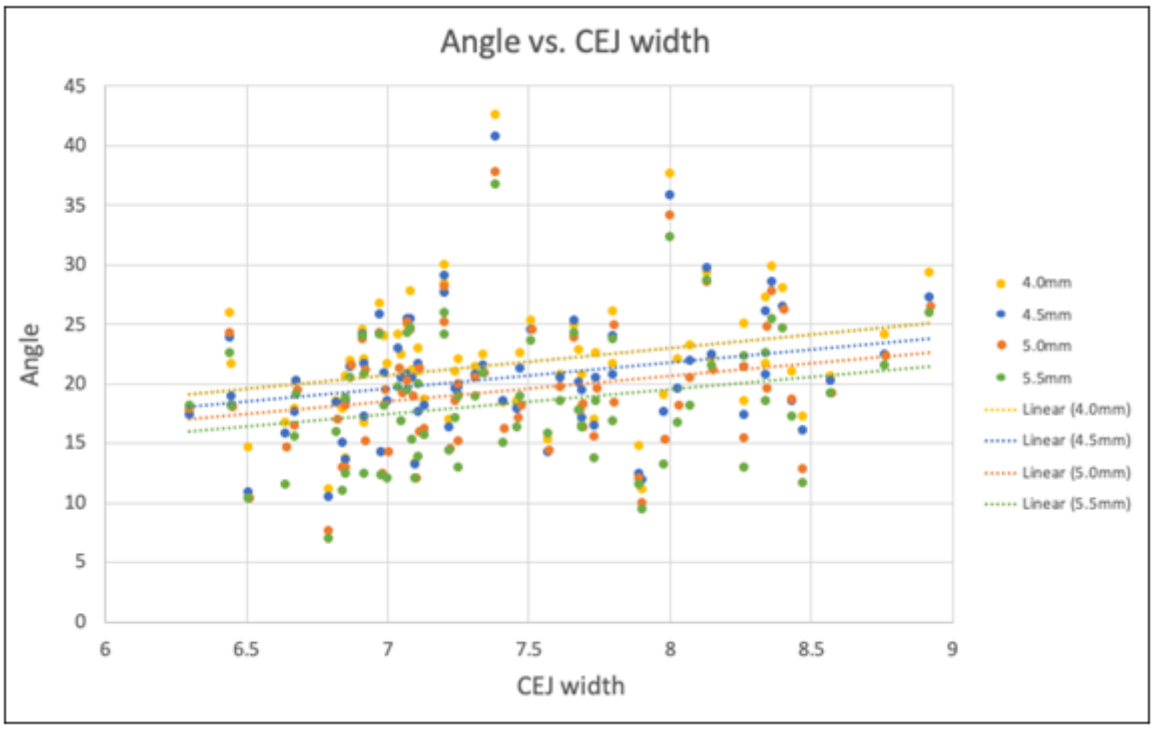

Figure 3

Tangent angles at 4.00 mm (*P* = 0.027), 4.50 mm (*P* = 0.032), 5.00 mm (*P* = 0.037), and 5.50 mm (*P* = 0.047) correlate with CEJ width. Linear trendlines for each location are provided